Increasing intensity of extreme global heatwaves: the crucial role of metrics

Emmanuele Russo[1] and Daniela I.V. Domeisen[2]

[1]Swiss Federal Institute of Technology in Zurich
[2]ETH Zurich

November 22, 2022

Abstract

Many indices have been defined to estimate the intensity of a heatwave. However, these indices are often used indiscriminately, without sufficient consideration of their possible different results and of the challenges that this poses to a proper characterization and comparison of events.

This study, by comparing four different indices applied to reanalyses data, shows that the choice of heatwave intensity metrics has important effects on the detection of the most intense events for the period 1950-2021, with indices based on cumulative values of a target variable that must be preferred over the ones relying on temporal averages. Under these considerations, one of the given indices is additionally selected for the study of heatwaves of the period 1950-2021, showing that heatwaves that were unlikely before 1986 have become up to ten times more usual and up to three times more intense during recent times.

Increasing intensity of extreme global heatwaves: the crucial role of metrics

Emmanuele Russo[1] and Daniela I.V. Domeisen[2,1]

[1]Institute for Atmospheric and Climate Science, ETH Zurich, Zürich, Switzerland
[2]Université de Lausanne, Lausanne, Switzerland

Key Points:

- ERA5-Land is in good agreement with Berkeley-Earth and JRA-55 only over part of the Northern Hemisphere for daily maximum temperatures
- The most intense heatwaves of 1950-2021 change if considering intensity indices either based on cumulative or averaged values
- The most intense heatwaves of 1950-1985 have become up to ten times more usual and up to three times more intense during recent years

Corresponding author: Emmanuele Russo, `emmanuele.russo@env.ethz.ch`

Abstract

Many indices have been defined to estimate the intensity of a heatwave. However, these indices are often used indiscriminately, without sufficient consideration of their possible different results and of the challenges that this poses to a proper characterization and comparison of events. This study, by comparing four different indices applied to reanalyses data, shows that the choice of heatwave intensity metrics has important effects on the detection of the most intense events for the period 1950-2021, with indices based on cumulative values of a target variable that must be preferred over the ones relying on temporal averages. Under these considerations, one of the given indices is additionally selected for the study of heatwaves of the period 1950-2021, showing that heatwaves that were unlikely before 1986 have become up to ten times more usual and up to three times more intense during recent times.

Plain Language Summary

This work sets the basis for a more consistent and unified use of metrics for the assessment of heatwave intensity. Following the evidence of previous studies, here we confirm that the way heatwave intensity is calculated might lead to completely different outcomes, such as in the case of the most intense events occurring globally over the period 1950-2021: indices of heatwaves magnitude have to be based on cumulative values of the anomalies of a target variable rather than on temporal averages. Additionally, considering a metric based on cumulative values of standardized anomalies of daily maximum temperatures, the trends of very extreme heatwaves over the period 1950-2021 show that for all of the considered regions, what was rarely recorded in the period 1950-1985 has become up to ten times more likely and up to three times more intense over the years 1986-2021.

1 Introduction

Heatwaves are defined as extended periods of extreme warm temperature anomalies (Perkins & Alexander, 2013; Perkins-Kirkpatrick & Lewis, 2020). They are considered to be one of the most harmful natural hazards, with serious implications for human health (Kovats & Kristie, 2006; Fischer & Schär, 2010; Williams et al., 2012; Cusack et al., 2011; López-Bueno et al., 2021), infrastructure (Forzieri et al., 2018; Maggiotto et al., 2021; Stone Jr et al., 2021), the economy (García-León et al., 2021) and natural ecosystems (Breshears et al., 2021).

Heatwaves are normally assessed through measures of their intensity, frequency, duration and spatial extent (Perkins-Kirkpatrick & Lewis, 2020). There exists a plethora of different metrics for characterizing each of these features, often tailored to the specific needs of a given study, depending on the sector and area of the application. This heterogeneity in the use of metrics does not always allow for a comprehensive understanding of how heatwaves differ over time as well as by region. For this reason, many studies have called for a unified and consistent way of defining heatwaves (Russo & Sterl, 2011; Perkins & Alexander, 2013; Russo et al., 2015; Perkins-Kirkpatrick & Lewis, 2020).

One parameter of particular importance for the characterization of heatwaves and their impact is the heatwave magnitude or intensity. This heatwave characteristic is relevant since it is directly linked to the severity of heatwave impacts on natural ecosystems (Iwasaki & Noda, 2018). To assess the magnitude of a heatwave, a wide range of indices has been proposed that can be classified into two groups: 1. considering metrics based on temporal averages of a target variable (Cowan et al., 2014; Holbrook et al., 2022; Schaeffer & Roughan, 2017; Yu et al., 2020; Cueto et al., 2010; Perkins et al., 2012); 2. relying on cumulative values of the anomalies of a given variable calculated over the duration of an event (Russo & Sterl, 2011; Russo et al., 2014, 2015, 2016). The intensity of a heatwave for a specific location is related to the duration of the event (Russo et al., 2014). While metrics based on cumulative values consider both the magnitude and the duration of heatwaves jointly, averaging does not allow for a direct comparison of heatwaves of different length. However, metrics for the characterization of heatwave intensities based on cumulative or averaged values are often used indiscriminately. There is therefore a need to better assess the effects of the two approaches, highlighting possible differences that might alter any conclusion relevant for the detection, prediction and understanding of heatwaves.

In this study, the most intense heatwaves occurring over the period 1950-2021 are detected and characterized at a global scale by means of four different heatwave magnitude indices either based on cumulative or averaged values of temperature-based variables. The main goal of this study is to identify possible inconsistencies between the two families of metrics and to set the basis for a more consistent and unified use of indices. All the presented analyses are conducted on the ERA5-Land reanalysis dataset (Muñoz-Sabater et al., 2021). Prior to the index calculation, ERA5-Land is evaluated against the Berkeley-Earth and JRA-55 datasets, to identify areas where it can be considered more reliable in terms of interannual variability of daily maximum temperatures. Then, the maximum heatwaves intensity and the year in which these events occur over the period from 1950 to 2021, according to ERA5-Land, are determined using the four considered indices, with the goal of highlighting different conclusions arising from the use of different approaches. Finally, in a last step, differences between the first and the second half of the considered study period in terms of occurrence and magnitude of very extreme heatwaves are investigated for one of the proposed metrics and specific regions.

2 Methods

2.1 Data

The analyses presented in this study are based on daily maximum temperature for the period 1950-2021 from the ERA5-land reanalysis dataset on a regular grid at a spatial resolution of 0.25°longitude $\times$ 0.25°latitude.

ERA5-Land provides hourly information of surface variables at a spatial resolution of ∼9km. The data is derived from a single simulation with the ECMWF *Carbon Hydrology-Tiles scheme for Surface Exchanges over Land (CH-TESSEL)* model, forced by meteorological fields of the lowest atmospheric level of the ERA5 reanalysis (Hersbach et al., 2020), with an additional lapse-rate correction (Muñoz-Sabater et al., 2021). The model version employed for the production of ERA5-Land is very similar to the one used for ERA5, but with an updated parameterization of the soil thermal conductivity after Peters-Lidard et al. (1998), technical fixes improving the conservation of soil moisture balance and additional improvements for the calculation of potential evapotranspiration fluxes. These improvements do not lead to remarkable differences between ERA5-Land and ERA5, given the fact that they still share common and similar parameterizations of land processes (Muñoz-Sabater et al., 2021). The main added value of ERA5-Land over ERA5 is attributable, according to Muñoz-Sabater et al. (2021), to the non-linear dynamical downscaling with corrected thermodynamic input, allowing for example to better discriminate between land and sea points over coastal areas.

The reliability of ERA5-Land in terms of daily maximum temperatures is assessed here against two additional datasets: the gridded Berkeley-Earth observational dataset (Rohde et al., 2013) (BE hereafter) and the Japanese reanalysis dataset JRA-55 (Kobayashi et al., 2015). These datasets are chosen as they have a temporal coverage similar to ERA5-Land, with BE starting in 1950 and JRA-55 in 1958. Daily gridded values of maximum temperatures are available on a regular grid with a spatial resolution of 1°longitude $\times$ 1°latitude for BE and of 1.25°longitude $\times$ 1.25°latitude for JRA-55. For the comparison against these two other datasets, ERA5-Land is first upscaled onto the respective coarser-resolution grids from each dataset, through conservative remapping.

All the employed datasets cover the entire globe. However, in this study only the data between -80°to 80°N are considered. Additionally, it is important to note that for the comparison of ERA5-Land against JRA-55, daily maxima are obtained from 6-hourly instead of from 1-hourly data, corresponding to the JRA-55 temporal resolution.

2.2 Heatwave Definition

Heatwave events are defined here as at least 3 consecutive days with temperatures exceeding a given threshold. Similar to the definition used in Russo et al. (2015) and Perkins-Kirkpatrick and Lewis (2020), for a specific day d, here the threshold $Tr90_d$ is defined as the 90th percentile of daily maximum temperatures, in a sliding window of 30 days around the considered day of a year, over a 30-year reference period.

We select the period from 1961 to 1990 as our reference period, as this period is often considered as a reference for long-term climate change assessments (Tavakol et al., 2020).

2.3 Heatwave Magnitude Indices

With the goal of identifying possible differences arising from the application of metrics using cumulative or averaged values of temperature-based variables, four different ways of assessing heatwave intensity are considered here, two for each of the two given classes. The first one is based on the magnitude assessment of single heatwave events over a season, while the other three jointly consider all the days characterized by a heatwave during an entire season. Below, the four indices are described in detail.

2.3.1 HWMId

The HWMId of Russo et al. (2015) is calculated as the sum, for a single point, of the daily magnitude index (M_d) over each of the days composing a heatwave event. For computing M_d, first anomalies of daily maximum temperatures for a given day d are computed with respect to the 25^{th} percentile of yearly maxima over the reference period. Then, the anomalies are standardized by the interquartile range (IQR) of the yearly maxima of daily maximum temperatures over the reference period, allowing for a comparison of different points in space characterized by different interannual variability:

$$M_d(T_d) = \left\{ \begin{array}{ll} \frac{T_d - T_{30y25p}}{T_{30y75p} - T_{30y25p}} & if\ T_d > T_{30y25p} \\ 0 & if\ T_d \leq T_{30y25p} \end{array} \right\} \tag{1}$$

where T_d is the daily maximum temperature on day d of a heatwave, T_{30y25p} and T_{30y75p} are, respectively, the 25^{th} and 75^{th} percentile values of the time-series composed of 30-year yearly maxima of daily temperatures for the reference period 1961–1990.

The methodology introduced by Russo et al. (2015) was designed for characterizing heatwaves over Europe, where the annual maxima of daily temperatures generally occur in boreal summer. Here, considering almost the entire globe, it is important to acknowledge that over other areas yearly maxima might take place at different times of the year. Therefore, similarly to Russo et al. (2016), the presented analyses are conducted separately for each season of the year (e.g., June July August (JJA)). In order to include heatwaves that start in a season and finish in another, periods of five months are selected around each 3-month season for the definition of heatwaves, with an additional month at the beginning and at the end of their classical definition (e.g. May to September (MJ-JAS) for boreal summer). Then, to avoid counting single events twice, heatwaves are assigned to a specific season depending on the largest number of days they have in the three central months of each season.

2.3.2 Cumulative Heat

The cumulative heat defined in Perkins-Kirkpatrick and Lewis (2020) is given by the sum of the anomalies with respect to the threshold in daily maximum temperatures of section 2.2, over all days characterized by a heatwave in each of the seasons s of the considered study period:

$$HEATcum_{y_s} = \sum_{d=1}^{n_{y_s}} T_d - Tr90_d \tag{2}$$

where y indicates the given year, d the heatwave day of a season, n the total number of heatwave days in that season and $Tr90_d$ the 90^{th} percentile threshold for a given day, as defined above.

2.3.3 AVI

The heatwave average intensity (AVI) of Perkins-Kirkpatrick and Lewis (2020) is the average temperature calculated over all the heatwave days of a season, for each year of the considered period:

$$AVI_{y_s} = \frac{\sum_{d=1}^{n_{y_s}} T_d}{n_{y_s}} \tag{3}$$

where, similarly to equation 2, y and s are, respectively, the considered year and season, d the given day of a heatwave, and n_{y_s} the total number of heatwave days in that season.

2.3.4 AVA

The heatwave Average Anomalies (here referred to as AVA) index is derived from the study of Perkins-Kirkpatrick and Lewis (2020) and represents the average of the temperature anomalies with respect to the corresponding threshold, calculated over all the heatwave days of a given season:

$$AVA_{y_s} = \frac{\sum_{d=1}^{n_{y_s}} T_d - Tr90_d}{n_{y_s}} \tag{4}$$

where, again, y and s are, respectively, the considered year and season, d is the given heatwave day and n_{y_s} the total number of heatwave days in that season.

3 Results

Prior to the comparison of the considered indices applied to daily temperature maxima derived from ERA5-Land, an evaluation of ERA5-Land against BE and JRA-55 is conducted in terms of the interannual variability of seasonal maxima of the target variable for each grid point of the domain. This allows us to better understand where the data can be considered more reliable for the estimation of the most intense heatwaves of a given period.

Fig. 1 shows global maps of the Spearman rank correlation calculated over each grid point of the domain at a 1°longitude × 1°latitude spatial resolution, between the

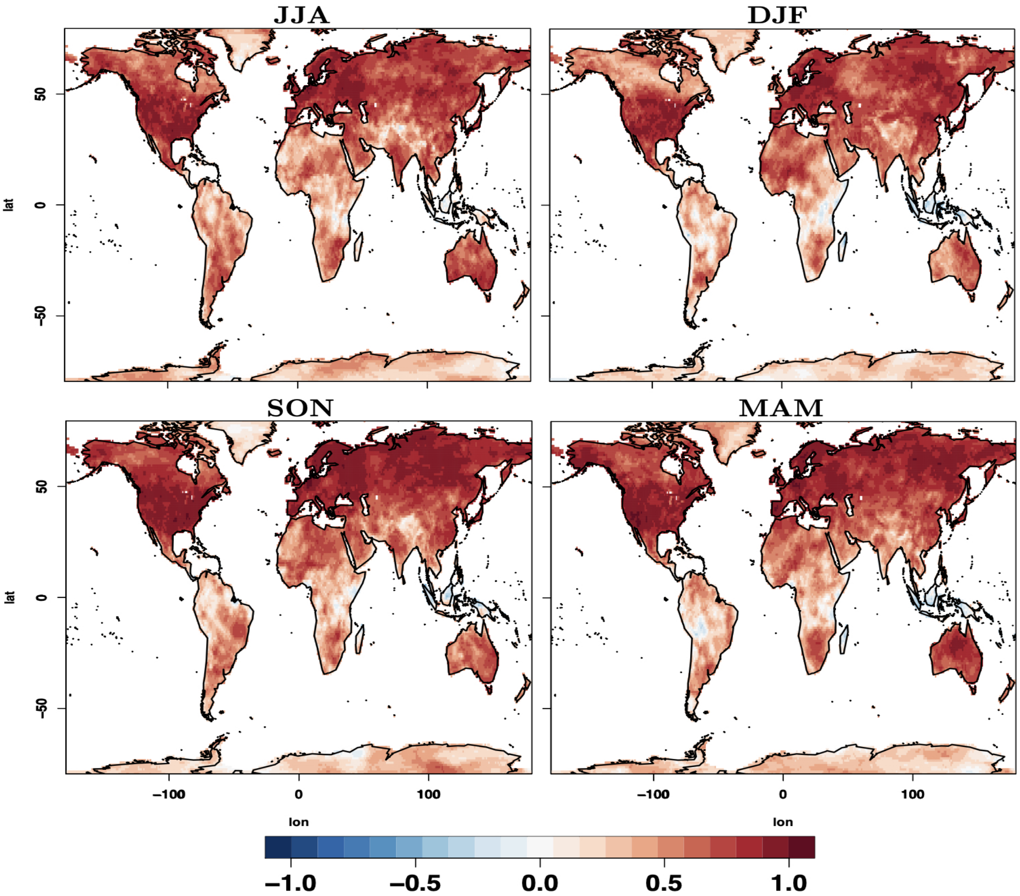

Figure 1. Spearman correlation calculated for the amplitude of the seasonal maxima of daily maximum temperatures between ERA5-Land and Berkeley Earth, over the period 1950-2021, at 1×1°resolution. The correlation is calculated for each season separately (from top to bottom: JJA, DJF, SON and MAM).

time-series of seasonal maxima of daily maximum temperatures derived from ERA5-Land and BE, for all four seasons of a year. In all seasons, the two datasets show a good agreement in terms of the considered variable between 30°N and 65 °N, while the agreement between the datasets in the continental Southern Hemisphere is lower. For the tropical regions of South America and Africa, even negative correlations are evident in some cases between the two datasets. Regions characterized by complex topography, such as Greenland, Antarctica and the Tibetan plateau, also show very low correlation between ERA5-Land and BE, with values generally lower than +0.2 for all seasons. Northern North America exhibits a remarkably low correlation (below +0.5) in DJF. Also, Western Australia shows a lower correlation in DJF and SON than in the other seasons. The same analyses conducted between ERA-Land and JRA-55 produce similar results, with Africa, South America and Antarctica presenting correlations lower than 0.5 for almost all grid points, and in all seasons (see supplements, Fig. S1). This agrees with findings comparing global daily maximum temperatures from ERA5 against JRA-55 (Thompson et al., 2022).

In a next step, daily maximum temperatures from the ERA5-Land dataset at a spatial resolution of 0.25°longitude × 0.25°latitude are used to determine the most intense heatwaves of the period 1950-2021 and the year in which they occur, according to the four indices defined in section 2.3. The goal is to investigate whether and how the detection of the most extreme events changes when considering different metrics. Fig. 2 shows the maximum values of the four given indices, for each season separately, over the period 1950-2021. The points for which the correlation between seasonal maxima of daily maximum temperatures calculated between ERA5-Land and BE is lower than +0.5 are shaded in gray. Fig. 2 illustrates how the AVI has a completely different pattern of the maxima with respect to the other indices. This is due to the fact that the AVI considers absolute temperatures: for this index it is not possible to properly compare extremes over regions characterized by different seasonal cycles (also relevant for heatwave prediction (De Perez et al., 2018)). Considering the indices based on temperature anomalies, the AVA, relying on temporal averages, has a different pattern of the maxima with respect to the two other indices (i.e., HWMId and HEATcum). In particular, the HWMId and HEATcum show maximum values over corresponding areas, in all seasons, except for SON when HEATcum shows much larger values over the high northern latitudes. In general, more pronounced maxima are evident over the higher latitudes of the Northern Hemisphere for HEATcum than for HWMId. This is true also when considering the HWMId calculated over all the heatwave days of a season, as for HEATcum (see supplements, Fig. S2), confirming that these differences are due to the consideration of standardized values of the anomalies for the HWMId. In JJA, HWMId and HEATcum both have some of their highest values over Western Russia, which can be associated with the extreme summer heatwave of 2010 (Russo et al., 2014, 2015). On the other hand, in JJA values of AVA over this region are not very pronounced and other areas show considerably larger values in terms of the defined metric. This behavior is noticeable also when considering the extreme values of HWMId and HEATcum for Central Africa and South America, in JJA, SON and MAM (where ERA5-Land exhibits a strong disagreement with respect to the other datasets): these anomalous events almost disappear in the case of AVA.

Another interesting way to look at possible differences arising from the application of the different metrics is by considering the years when the corresponding event with maximum magnitude occurs over the period 1950-2021. A very important result evident from Fig. 3 is that while the maps of the year when the maxima in the given metrics occur are pretty similar in the case of HWMId and HEATcum, the AVI and AVA show a very different spatial distribution. While for the first two indices (shown in the first two columns), for more than 70% of the land areas the most intense heatwave event occurs during the last 36 years of the considered period, in the other two more than 50% of the most extreme events take place before the year 1986. In particular, the differences between AVA and HEATcum are considerably larger than the differences between HWMId and HEATcum in all cases, even though HWMId is not only based on standardized anomalies, but it also considers cumulative values over single events instead of an entire season. Hence, the conclusions on the most intense events and the years in which they occur that can be drawn from the two groups of indices are substantially different. This demonstrates that metrics assessing heatwave intensity based either on temporal means or cumulative values cannot be used indiscriminately.

Finally, the trends in the intensity of single heatwave events are investigated over the entire period 1950-2021. The HWMId allows us to calculate heatwave intensity for single events, while at the same time providing a standardized measure useful for the comparison across time and space. Hence, for the next analysis, the HWMId of single heatwave events over the period 1950-2021 is calculated for selected subregions of the Northern Hemisphere, namely Central North America (CNA), Europe (EUR) and Northern Asia (NAS, see supplements, Fig. S3), for which the ERA5-Land shows a better agreement with other datasets in terms of the interannual variability of daily maximum temperatures. Over each of these regions, for each season, the changes in the number of very extreme events and their intensities between two periods of 36 years (hereafter referred to as Early Period (EP) and Late Period (LP), respectively), the first starting in 1950

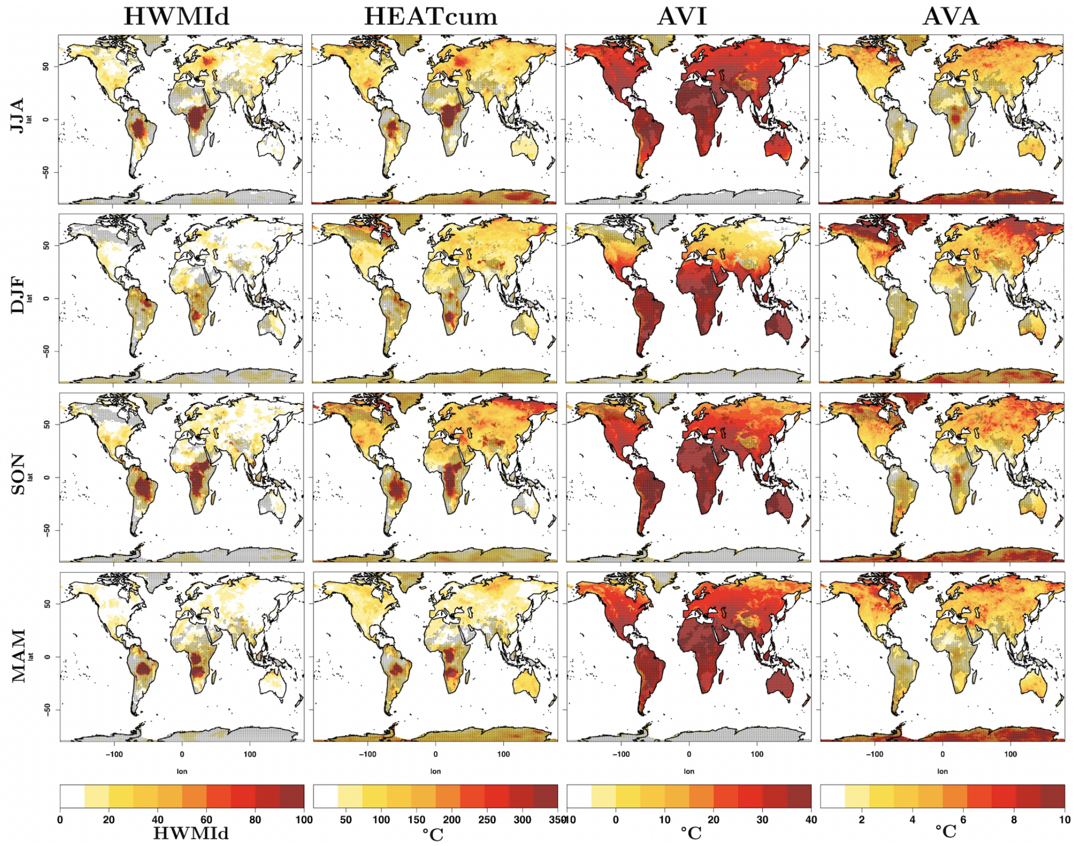

Figure 2. From top to bottom, maximum values of JJA, DJF, SON and MAM for (from left to right) HWMId, HEATcum, AVI and AVA, applied to ERA5-Land daily maximum temperatures over the period 1950-2021.

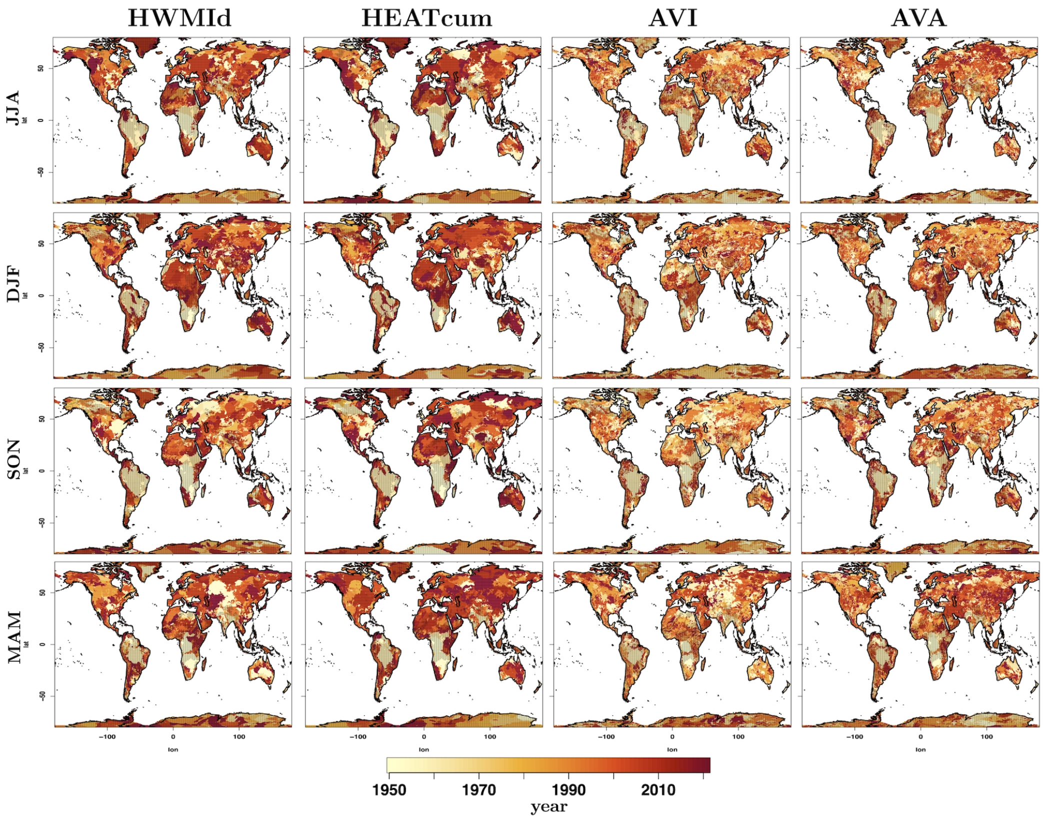

Figure 3. Year when the maximum values of, from left to right, HWMId, HEATcum, AVI and AVA occur over the period 1950-2021, according to ERA5-Land daily maximum temperatures. From top to bottom, the seasonal values derived for JJA, DJF, SON and MAM are shown.

and the second in 1986 (except DJF where periods of 35 years are considered, starting in 1952 and 1987, respectively) are investigated. A heatwave event is considered as very extreme when its corresponding HWMId value is larger than the 99.9^{th} percentile of the values calculated for all the points of the considered subdomain over the period 1950-1985.

Fig. 4 shows the number of very extreme heatwaves for different values of HWMId, for all seasons and considered regions. In general, a higher number and more intense extreme heatwaves are evident over the period 1986-2021 compared to 1950-1985, in all seasons and regions. In CNA, the maximum intensities are higher during LP than in EP, for all seasons, up to almost two times in JJA. The number of very extreme events also strongly increases in this region during LP compared to EP, up to almost four times more in MAM. In CNA, during LP, only a small number of events exceeds the maximum intensity of heatwaves during EP, for a maximum number of 118 times in JJA. In NAS, the maximum intensities are also more pronounced during the most recent of the two periods, for all seasons, with values up to more than three times higher in JJA. For NAS the number of very extreme events increases by more than a factor of two over LP, in all seasons, with an exceptional increase by a factor greater than five in DJF and JJA. For the same region, during LP, a large amount of events exceeds the highest intensity of EP, for a maximum of 262 times in DJF and 599 in JJA. The largest changes between the two periods in both the number of events and their maximum magnitudes are evident for Europe, in particular in JJA, DJF and MAM. Here an event considered very extreme during EP occurs at least four times more often during the most recent period in JJA and MAM, and more than ten times more often in DJF. The maximum HWMId value registered over the two periods for EUR is almost the same in SON, approximately twice in DJF and up to three times more in MAM and JJA during recent times. Additionally, for EUR, in an exceptionally high number of cases the maximum intensity of the period 1950-1985 is exceeded during the most recent period, up to 761 times in DJF and almost 2000 times in JJA.

4 Conclusions

Several studies have called for a more unified definition and assessment of heatwave characteristics. Nonetheless, a plethora of different approaches is still employed for the study of heatwaves. In particular, concerning heatwave intensity, metrics based on cumulative or averaged values of a target variable are often used indiscriminately.

The results presented in this study show that the selection of metrics for the assessment of heatwave intensities needs extreme caution: the year and spatial distribution of the most intense events over the period 1950-2021, as calculated from daily maximum temperatures from the ERA5-Land reanalysis, change remarkably when considering four different indices belonging to two families of metrics, one based on temporal averages and the other on cumulative values. The use of metrics based on cumulative values should be preferred over the ones relying on temporal averages since, as already suggested by Russo et al. (2014), assessing intensity through averaged values does not allow for an unequivocal comparison of the magnitude of events with differing length. One simple example that could help in clarifying this point further is by considering two different heatwaves, the first one, HW1, lasting three days and the second, HW2, lasting four days. Supposing that HW1 has a value of the anomalies for each of the three heatwave days of +3°C, and HW2 has a value of the anomalies of +3°C for three heatwave days and of 2°C for the fourth one, when considering the average value of the anomalies the event HW1 will misleadingly be considered more intense than HW2. An additional important consideration on the reason to prefer cumulative values over averaged ones in the computation of heatwaves intensity is that, from an impact point of view, it is important to assess accumulated excess heat experienced over a given period of time (Perkins-Kirkpatrick & Lewis, 2020).

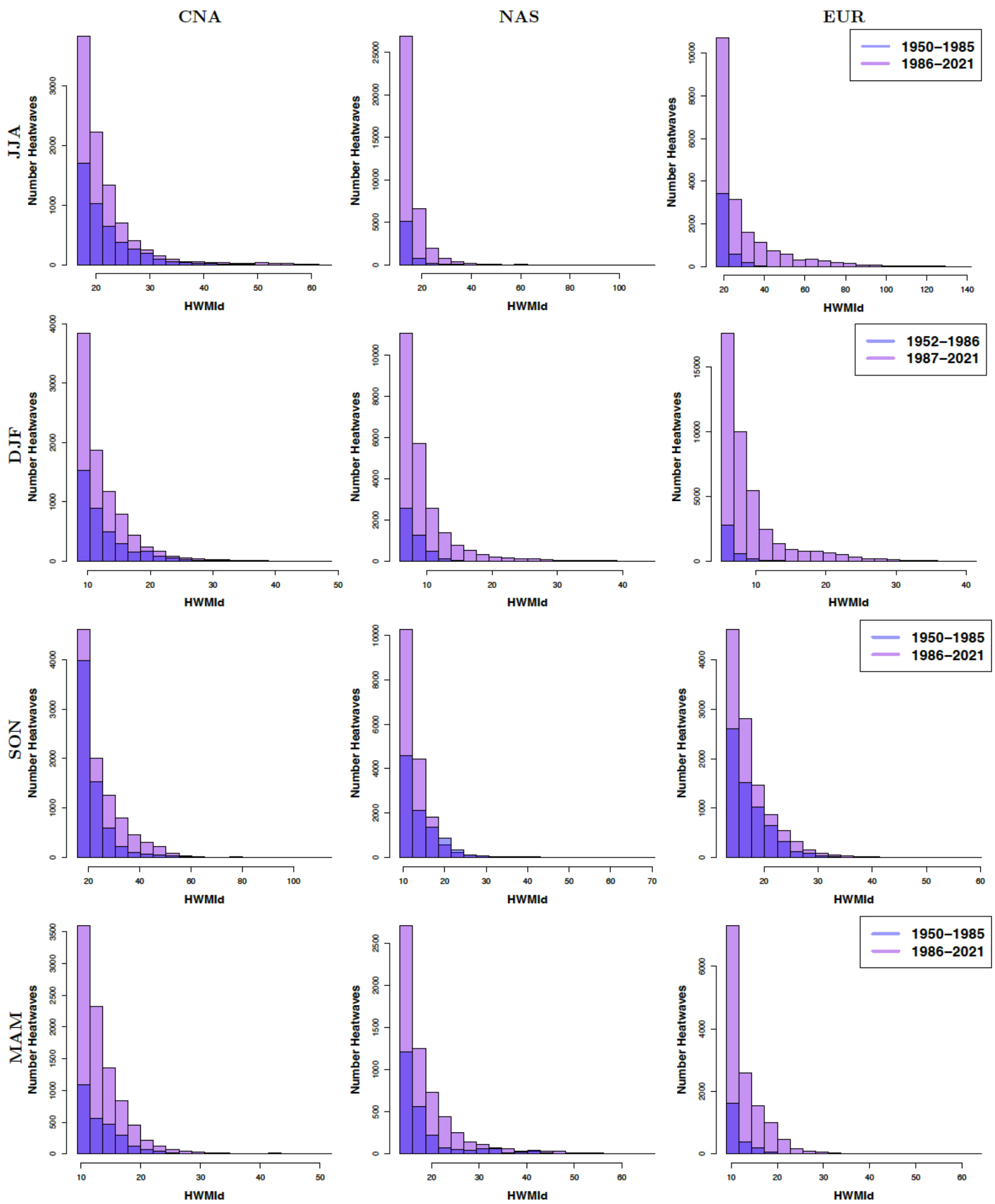

Figure 4. Number of heatwaves with intensities higher than the 99.9^{th} percentile of HWMId calculated from ERA5-Land over the period 1950-1985, for Central North America (CNA), Northern Asia (NAS) and Northern Europe (NEU). From top to bottom, results for, respectively, JJA, DJF, SON and MAM, are represented through *light blue* bars for the period 1950-1985 and in *purple* for the period 1986-2021. The regions where the bars for both periods overlap are highlighted in darker purple.

The presented analyses additionally include, for the first time, an evaluation of ERA5-Land in terms of the interannual variability of seasonal maxima of daily maximum temperatures against the Berkeley Earth gridded observations and the JRA-55 reanalysis product, at a global scale. For all seasons, over a large part of the Southern Hemisphere, ERA5-Land exhibits correlations against the other datasets lower than 0.5, and in some cases even negative values. The areas for which ERA5-Land is in better agreement with the other two datasets, in all seasons, are Europe, Central North America and Northern Asia.

For these three regions where ERA5-Land is in better agreement with the other datasets, a grid-point-based analysis of the trends of heatwaves over the distinct periods 1950-1985 and 1986-2021 is performed, considering a cumulative index for heatwave intensity based on standardized anomalies of maximum daily temperatures. In many of the considered seasons and regions there is a clear increase in the number and intensity of heatwaves over the recent years 1986-2021, compared to what was considered very extreme during the period 1950-1985. Europe is the area where the most pronounced changes between the two periods emerge, with the total number of very extreme events increasing more than ten-fold in boreal winter, and the maximum intensity reaching values up to three times higher in summer during the most recent times: what was virtually impossible during the period 1950-1985 has become more common and extreme in the successive 36 years.

This study sets the basis for a more unified use of metrics for the calculation of heatwave intensity, at the same time providing an analysis of the trends in the number and intensity of very extreme events over the period from 1950 to 2021, for selected regions, revealing exceptionally severe changes in heatwaves.

5 Open Research

5.1 Data Availability Statement

The ERA5-Land hourly near surface temperature data used for the computation of the different heatwave indices proposed in the study are available at the ECMWF Copernicus Climate Change Service (C3S) Climate Data Store (CDS) via `https://doi.org/10.24381/cds.e2161bac`. The Berkeley-Earth gridded daily maximum temperature observational data are available at http://berkeleyearth.org/data/. 6-hourly JRA-55 near-surface temperature data are available at the Research Data Archive of the National Center for Atmospheric Research, Computational and Information Systems Laboratory, via `ds628.0|DOI:10.5065/D6HH6H41`.

Acknowledgments
This project has received funding from the European Research Council (ERC) under the European Union's Horizon 2020 research and innovation programme (grant agreement No. 847456). Support from the Swiss National Science Foundation through project PP00P2_198896 to D.D. is gratefully acknowledged. We additionally acknoledge the IAC-Landclim group of the ETH Zurich for retrieving the ERA5-Land data.

References

Breshears, D., Fontaine, J., Ruthrof, K., Field, J., Feng, X., Burger, J., … Hardy, G. (2021). Underappreciated plant vulnerabilities to heat waves. *New Phytologist*, *231*(1), 32–39.

Cowan, T., Purich, A., Perkins, S., Pezza, A., Boschat, G., & Sadler, K. (2014). More frequent, longer, and hotter heat waves for australia in the twenty-first century. *Journal of Climate*, *27*(15), 5851–5871.

Cueto, R. G., Martínez, A., & Ostos, E. (2010). Heat waves and heat days in an arid city in the northwest of mexico: current trends and in climate change scenarios. *International journal of biometeorology*, *54*(4), 335–345.

Cusack, L., de Crespigny, C., & Athanasos, P. (2011). Heatwaves and their impact on people with alcohol, drug and mental health conditions: a discussion paper on clinical practice considerations. *Journal of advanced nursing*, *67*(4), 915–922.

De Perez, E., Van Aalst, M., Bischiniotis, K., Mason, S., Nissan, H., Pappenberger, F., … Van Den Hurk, B. (2018). Global predictability of temperature extremes. *Environmental Research Letters*, *13*(5), 054017.

Fischer, E., & Schär, C. (2010). Consistent geographical patterns of changes in high-impact european heatwaves. *Nature geoscience*, *3*(6), 398–403.

Forzieri, G., Bianchi, A., Silva, F., Herrera, M., Leblois, A., Lavalle, C., … Feyen, L. (2018). Escalating impacts of climate extremes on critical infrastructures in europe. *Global environmental change*, *48*, 97–107.

García-León, D., Casanueva, A., Standardi, G., Burgstall, A., Flouris, A., & Nybo, L. (2021). Current and projected regional economic impacts of heatwaves in europe. *Nature communications*, *12*(1), 1–10.

Hersbach, H., Bell, B., Berrisford, P., Hirahara, S., Horányi, A., Muñoz-Sabater, J., … others (2020). The era5 global reanalysis. *Quarterly Journal of the Royal Meteorological Society*, *146*(730), 1999–2049.

Holbrook, N., Hernaman, V., Koshiba, S., Lako, J., Kajtar, J., Amosa, P., & Singh, A. (2022). Impacts of marine heatwaves on tropical western and central pacific island nations and their communities. *Global and Planetary Change*, *208*, 103680.

Iwasaki, A., & Noda, T. (2018). A framework for quantifying the relationship between intensity and severity of impact of disturbance across types of events and species. *Scientific reports*, *8*(1), 1–7.

Kobayashi, S., Ota, Y., Harada, Y., Ebita, A., Moriya, M., Onoda, H., … Takahashi, K. (2015). The jra-55 reanalysis: General specifications and basic characteristics. *Journal of the Meteorological Society of Japan. Ser. II*, *93*(1), 5–48.

Kovats, R., & Kristie, L. (2006). Heatwaves and public health in europe. *European journal of public health*, *16*(6), 592–599.

López-Bueno, J., Navas-Martín, M., Linares, C., Mirón, I., Luna, M., Sánchez-Martínez, G., … Díaz, J. (2021). Analysis of the impact of heat waves on daily mortality in urban and rural areas in madrid. *Environmental research*, *195*, 110892.

Maggiotto, G., Miani, A., Rizzo, E., Castellone, M., & Piscitelli, P. (2021). Heat waves and adaptation strategies in a mediterranean urban context. *Environmental research*, *197*, 111066.

Muñoz-Sabater, J., Dutra, E., Agustí-Panareda, A., Albergel, C., Arduini, G., Balsamo, G., … Thépaut, J. (2021). Era5-land: A state-of-the-art global reanalysis dataset for land applications. *Earth System Science Data*, *13*(9), 4349–4383.

Perkins, S., & Alexander, L. (2013). On the measurement of heat waves. *Journal of climate*, *26*(13), 4500–4517.

Perkins, S., Alexander, L., & Nairn, J. (2012). Increasing frequency, intensity and duration of observed global heatwaves and warm spells. *Geophysical Research Letters*, *39*(20).

Perkins-Kirkpatrick, S., & Lewis, S. (2020). Increasing trends in regional heatwaves. *Nature communications*, *11*(1), 1–8.

Peters-Lidard, C., Blackburn, E., Liang, X., & Wood, E. (1998). The effect of soil thermal conductivity parameterization on surface energy fluxes and temperatures. *Journal of the Atmospheric Sciences*, *55*(7), 1209–1224.

Rohde, R., Muller, R., Jacobsen, R., Perlmutter, S., Rosenfeld, A., Wurtele, J., ... Mosher, S. (2013). Berkeley earth temperature averaging process, geoinfor. geostat.-an overview, 1, 2. *Geoinformatics Geostatistics An Overview*, *1*(2), 20–100.

Russo, S., Dosio, A., Graversen, R., Sillmann, J., Carrao, H., Dunbar, M., ... Vogt, J. (2014). Magnitude of extreme heat waves in present climate and their projection in a warming world. *Journal of Geophysical Research: Atmospheres*, *119*(22), 12–500.

Russo, S., Marchese, A. F., Sillmann, J., & Immé, G. (2016). When will unusual heat waves become normal in a warming africa? *Environmental Research Letters*, *11*(5), 054016.

Russo, S., Sillmann, J., & Fischer, E. (2015). Top ten european heatwaves since 1950 and their occurrence in the coming decades. *Environmental Research Letters*, *10*(12), 124003.

Russo, S., & Sterl, A. (2011). Global changes in indices describing moderate temperature extremes from the daily output of a climate model. *Journal of Geophysical Research: Atmospheres*, *116*(D3).

Schaeffer, A., & Roughan, M. (2017). Subsurface intensification of marine heatwaves off southeastern australia: the role of stratification and local winds. *Geophysical Research Letters*, *44*(10), 5025–5033.

Stone Jr, B., Mallen, E., Rajput, M., Gronlund, C., Broadbent, A., Krayenhoff, E., ... Georgescu, M. (2021). Compound climate and infrastructure events: how electrical grid failure alters heat wave risk. *Environmental Science & Technology*, *55*(10), 6957–6964.

Tavakol, A., Rahmani, V., & Harrington, J. (2020). Evaluation of hot temperature extremes and heat waves in the mississippi river basin. *Atmospheric Research*, *239*, 104907.

Thompson, V., Kennedy-Asser, A., Vosper, E., Lo, Y., Huntingford, C., Andrews, O., ... Mitchell, D. (2022). The 2021 western north america heat wave among the most extreme events ever recorded globally. *Science advances*, *8*(18), eabm6860.

Williams, S., Nitschke, M., Weinstein, P., Pisaniello, D., Parton, K., & Bi, P. (2012). The impact of summer temperatures and heatwaves on mortality and morbidity in perth, australia 1994–2008. *Environment international*, *40*, 33–38.

Yu, S., Yan, Z., Freychet, N., & Li, Z. (2020). Trends in summer heatwaves in central asia from 1917 to 2016: Association with large-scale atmospheric circulation patterns. *International Journal of Climatology*, *40*(1), 115–127.

Supporting Information for "Increasing intensity of extreme global heatwaves: the crucial role of metrics"

Emmanuele Russo[1] and Daniela I.V. Domeisen[2,1]

[1]Institute for Atmospheric and Climate Science, ETH Zurich, Zürich, Switzerland

[2]Université de Lausanne, Lausanne, Switzerland

Contents of this file

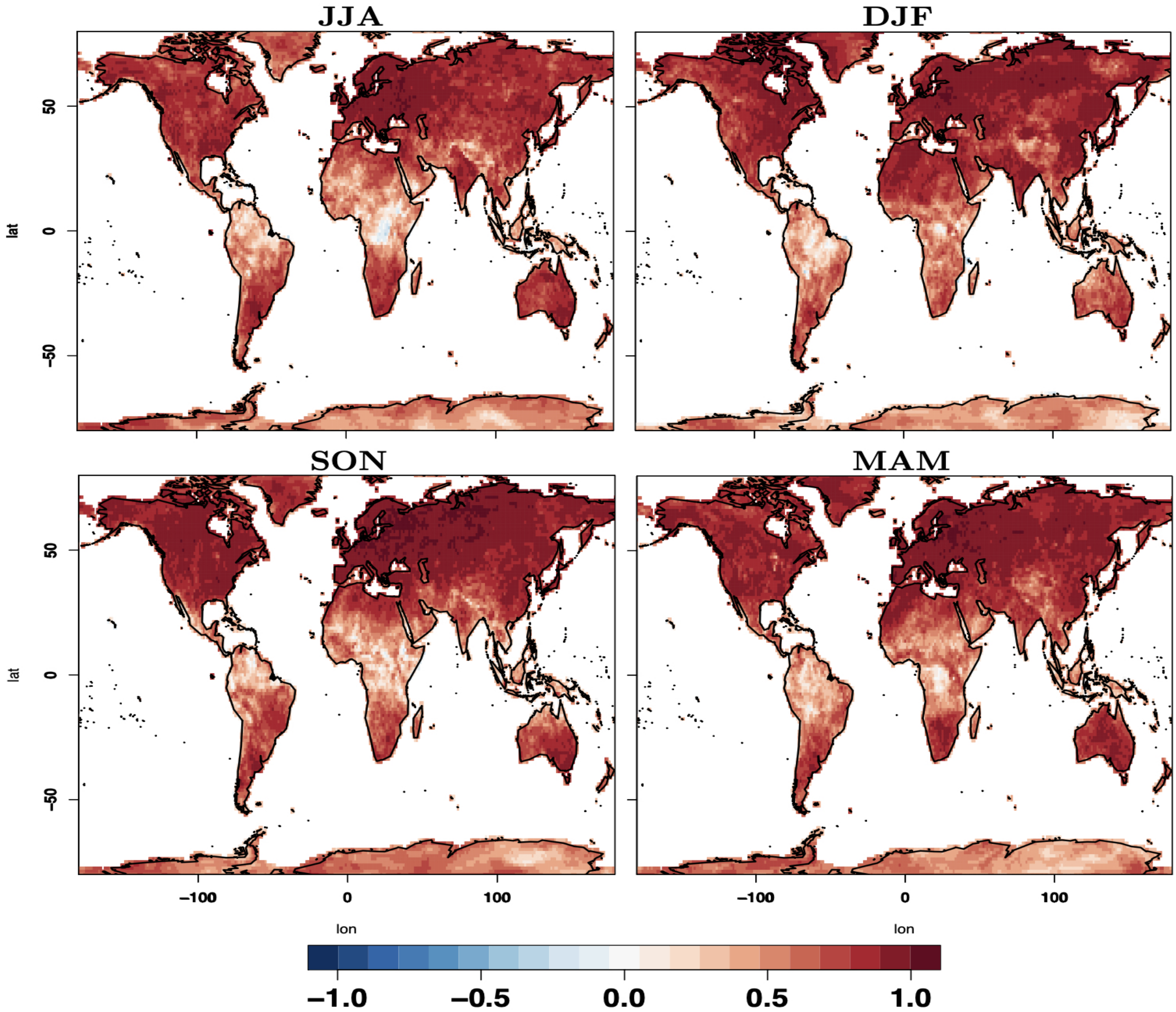

Figure S1. Spearman correlation calculated on seasonal maxima of daily temperature maximum derived from the ERA5-Land and the JRA-55 reanalysis dataset, over the period 1950-2021, at $1 \times 1°$resolution. The correlation is calculated for each season, considering only the given 3 months, separately. From top to bottom, the obtained results for, respectively, JJA, DJF, SON and MAM, are shown.

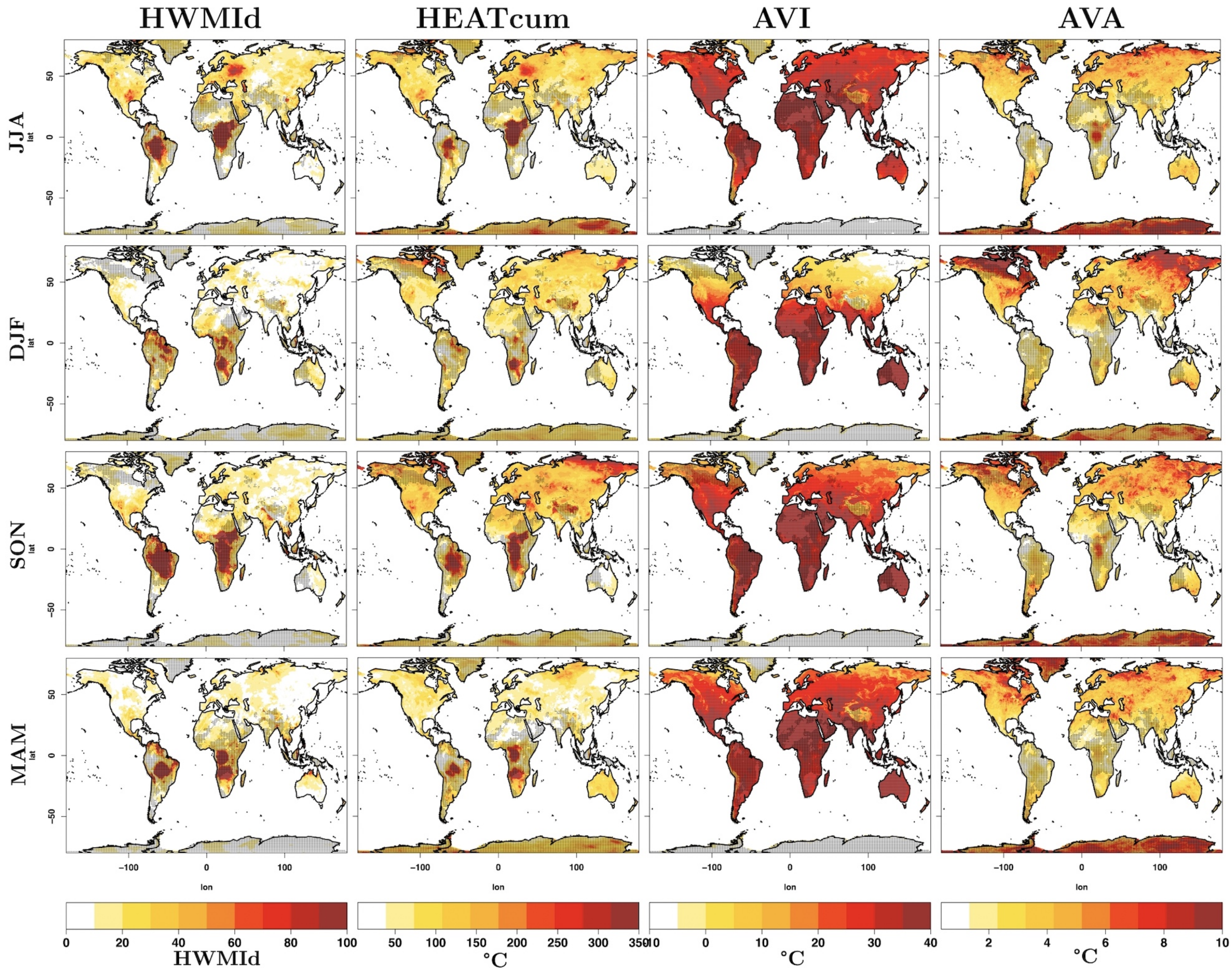

Figure S2. Maximum values of JJA HWMId calculated from ERA5-land daily maximum temperatures at high spatial resolution, over the period 1950-2021, but considering all the heatwave days of a season.

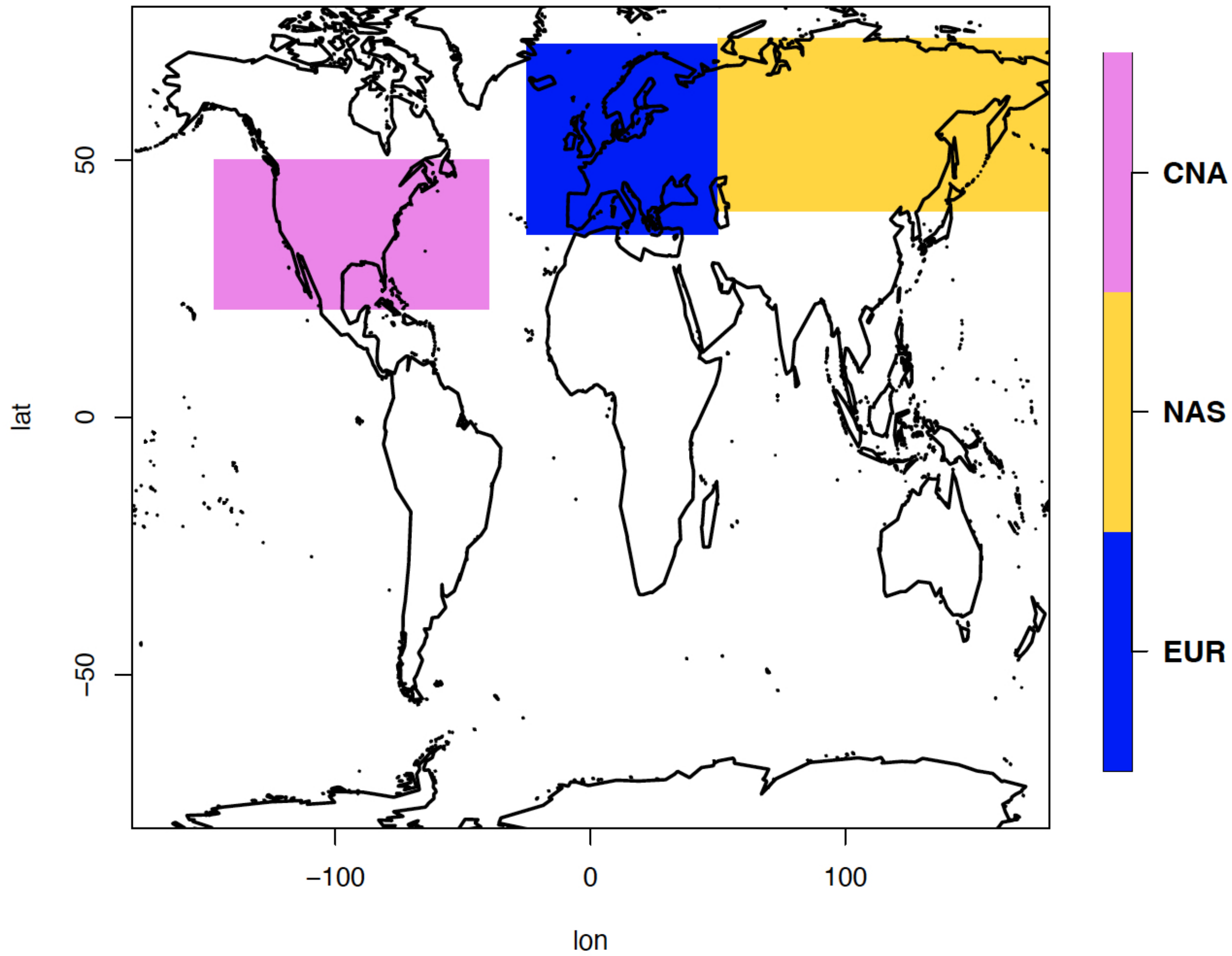

Figure S3. Domain Decomposition.

Table S1. Intensity indices definition.

INDEX	Definition	Description
HWMId	$\sum_{d=1}^{n_{HW}} M_d(T_d)$	Sum of anomalies of daily maximum temperatures for a given day d of a heatwave, standardized following eq. **??**
HEATcum	$\sum_{d=1}^{n_y} T_d - Tr90_d$	Sum of anomalies of daily maximum temperatures calculated over all the heatwave days of a given season.
AVI	$\frac{\sum_{d=1}^{n_y} T_d}{n_y}$	Mean value of daily maximum temperatures calculated over all heatwave days of a season.
AVA	$\frac{\sum_{d=1}^{n_y} T_d - Tr90_d}{n_y}$	Mean Value of the anomalies of daily maximum temperatures calculated over all heatwave days of a given season.